

A space-for-time framework for forecasting the effects of ocean stratification on zooplankton vertical habitat use and trait composition

Stephanie A. Matthews  1,2* Mark D. Ohman  1,2

¹California Current Ecosystem Long-Term Ecological Research Site, Scripps Institution of Oceanography, University of California San Diego, La Jolla, California, USA

²Integrative Oceanography Division, Scripps Institution of Oceanography, University of California San Diego, La Jolla, California, USA

Abstract

The effects of environmental change on zooplankton communities, and more broadly, pelagic ecosystems are difficult to predict due to the high diversity of ecological strategies and complex interspecific interactions within the zooplankton. Trait-based approaches can define zooplankton functional groups with distinct responses to environmental change. Analyses across multiple mesozooplankton groups can help identify key organizing traits. Here, we use the pronounced cross-shore environmental gradient within the California Current Ecosystem in a space-for-time substitution to test potential effects of ocean warming and increased stratification on zooplankton communities. Along a horizontal gradient in sea-surface temperature, water column stratification, and light attenuation, we test whether there are changes in zooplankton species composition, trait composition, and vertical habitat use. We employ DNA metabarcoding at two loci (18S-V4 and COI) and digital ZooScan imaging of zooplankton sampled in a Lagrangian manner. We find that vertical distributions of many mesozooplankton taxa shift to deeper depths in the cross-shore direction, and light attenuation is the strongest predictor of magnitude of change. Vertical habitat shifts vary among functional groups, with changes in vertical distribution most pronounced among carnivorous taxa. Herbivorous taxa remain associated with the chlorophyll maximum, especially in clear offshore waters. Our results suggest that increased stratification of this ocean region will lead to deeper depths occupied by some components of epipelagic mesozooplankton communities, and may result in zooplankton communities with more specialized feeding strategies, increased egg brooding, and more asexual reproduction.

Zooplankton are a central component of marine pelagic foodwebs, linking upwelling-driven primary production to economically important fisheries and protected mammal and bird species (Ruzicka et al. 2012). Because of their dispersal potential and relatively short generation times, zooplankton communities have the potential to respond rapidly to

environmental changes (Peijnenburg and Goetze 2013). Ocean stratification is predicted to increase as earth's climate warms (Li et al. 2020), due to warming temperatures and increased salinity (Capotondi et al. 2012). Increased ocean stratification has the potential to affect zooplankton directly (e.g., increased metabolic rates in warmer, more stratified areas) and indirectly (e.g., food limitation due reduced primary production). Zooplankton may also have mechanisms for mitigating the effects of increased stratification, such as plasticity in body size (Evans et al. 2020) or vertical migration to optimal habitats (Ohman and Romagnan 2016). Species-specific responses to ocean stratification that induce changes to zooplankton community composition, structure, richness, and diversity can have implications for higher trophic levels and result in changes to pelagic nutrient cycling and carbon export (Steinberg and Landry 2017). However, the effects on zooplankton communities as a whole are complex and difficult to predict, due to limited observations and the potential for interactions among species (Ratnarajah et al. 2023).

*Correspondence: samatthews@ucsd.edu

This is an open access article under the terms of the [Creative Commons Attribution-NonCommercial-NoDerivs](#) License, which permits use and distribution in any medium, provided the original work is properly cited, the use is non-commercial and no modifications or adaptations are made.

Additional Supporting Information may be found in the online version of this article.

Author Contribution Statement: S.M. developed the research questions, performed the laboratory work and data analyses, and wrote the manuscript. M.O. collected samples, assisted with interpretation of the data, and edited the manuscript.

One approach for projecting the effects of ocean stratification on zooplankton communities is to use existing spatial variability across an ecosystem as a proxy for predicted temporal trends within any one subregion. This space-for-time substitution (SFTS) is a widely adopted hypothesis in ecology (Pickett 1989). SFTS posits that biotic responses to climate drivers observed over a spatial gradient may be used to predict biotic changes in response to temporal changes in the same drivers. In the absence of time-series or experimental manipulations, SFTS provides a foundation for predicting future ecosystem states. The principle of SFTS can be traced to Charles Darwin's insights about formation of coral atolls as a progression from extinct volcanoes and fringing reefs (Damgaard 2019). While SFTS has been criticized for not considering historical legacy effects (Pickett 1989), other non-equilibrium conditions (Damgaard 2019), and for not always resolving causal relationships (Lovell et al. 2023), these same authors have endorsed its use with appropriate caution.

The California Current Ecosystem (CCE) is a highly productive eastern boundary current upwelling system and is the site of significant cross-shore environmental gradients, including in water column stratification. Nutrient rich waters are upwelled nearshore then advected away from the coast toward the cool, fresh, southward flowing California current, which is centered \sim 150–300 km offshore (Bograd et al. 2019; Chabert et al. 2021). Offshore, the California current is bounded by the warm highly stratified waters of the North Pacific Subtropical Gyre (Lynn and Simpson 1987; Thomson and Krassovski 2010). Nearshore, reduced stratification and increased nutrient availability supports higher primary production rates, resulting in a cross-shore gradient in biomass and community composition at multiple trophic levels (Kahru et al. 2015; Morrow et al. 2018). Along this gradient, zooplankton abundance and biomass are positively correlated with primary production rates and negatively correlated with ocean temperature (Valencia et al. 2018). In the CCE, climate change is expected to result in increased upper-ocean stratification within the next 25 years, primarily due to warming (Xiu et al. 2018). Despite some uncertainty regarding the spatial distribution of increased stratification and the ultimate effects on biogeochemistry in the region (Pozo Buil et al. 2021), zooplankton communities across the CCE will likely experience more stratified waters in the near future. Ohman et al. (2013) introduced SFTS for the present study region, illustrating how the covariability of existing spatial variations in nitracline depth and Chl *a* concentration over a horizontal scale of 350 km is comparable to their covariability over a temporal scale of 29 years. This existing gradient, from active upwelling to more stratified mesotrophic habitats, also provides a natural experiment for testing the potential effects of future warming and more stratified oceans on zooplankton.

To investigate how zooplankton communities change along a gradient in stratification, we use a trait-based approach. Previous studies have used a trait-based approach as a framework for examining functional groups and tradeoffs between ecological strategies (Litchman et al. 2013; Heneghan et al. 2020;

Martini et al. 2021). Variable effects of changing pelagic environments have been observed for zooplankton groups with different ecological constraints. Mesoscale changes in the dominant diet and feeding mode within the zooplankton community have been documented across ocean fronts within the CCE, with a shift from carnivory and omnivory toward particle-grazing communities in more productive regions (Ohman et al. 2012). Within copepod communities, functional groups defined by size, trophic group, feeding mode, myelination, and spawning strategy exhibit complementary biogeographic distributions on global latitudinal scales (Benedetti et al. 2022). Body size within copepods is strongly correlated with temperature and productivity, but environmental variability only explains \sim 50% of spatial patterns in marine copepods, indicating that additional variables, such as phylogenetic history, may play a role (Brun et al. 2016).

Trait-based analyses across multiple taxonomic groups can lead to novel insights of broad ecological patterns that are not apparent within the limited range of traits expressed within a single taxonomic group (Villarino et al. 2018). Trait-based analysis of multiple taxonomic groups of zooplankton can be aided by rapidly assessing community composition with metabarcoding. Metabarcoding uses a short region of DNA, termed a marker region, to identify the species present in a mixed sample. The method can be applied to a wide variety of ecosystems and sample types. For net-collected zooplankton samples, metabarcoding can be used to estimate the relative abundance of major taxonomic groups, particularly when multiple marker regions are analyzed (Matthews et al. 2021). Taxa detected by metabarcoding can further be assigned morphological and functional traits, when traits have previously been described for the species or taxonomic group.

Here, we use trait-based analyses of a paired metabarcoding and digital imaging dataset to analyze high resolution changes in species distribution, community composition, and shifts among zooplankton functional groups. We exploit a cross-shore environmental gradient in upwelling, stratification, productivity, and light attenuation across the CCE to test whether mesozooplankton community composition and vertical habitat use changes predictably with water column hydrographic structure. Specifically, we test 1) whether there are coherent changes in zooplankton species composition and vertical habitat use; and 2) whether the strength of such changes varies with zooplankton traits. These analyses will provide insight into the effects of environmental changes on different zooplankton functional groups and will help predict how zooplankton communities will respond to expected increased stratification in the future ocean.

Materials and methods

Study area

The CCE is a dynamic coastal region characterized by multiple ocean currents, including the California current, the

California undercurrent, and the inshore countercurrent, comprised of an admixture of Pacific Subarctic, Eastern North Pacific, and Pacific Equatorial water masses (Bograd et al. 2019). Our study targeted four distinct water masses, including two nutrient-limited sites with higher stratification and minimal light attenuation, one in the offshore region (Cycle 1) and one in the core California current (Cycle 2); one transition site characterized by moderate productivity and a phytoplankton community dominated by small ($< 1 \mu\text{m}$) phytoplankton cells (Cycle 3); and one coastal upwelling site with little stratification and elevated light attenuation, high productivity, and larger phytoplankton (Cycle 4) (Fig. 1; Morrow et al. 2018). “Cycles” refer to repeated daily measurements in a water parcel followed in a Lagrangian manner using a satellite-tracked mixed layer drifter (Landry et al. 2009; Ohman et al. 2013). Sampling was conducted between 22 April and 11 May 2016. During each Cycle, vertical profiles were resolved twice per day from continuous downcasts, using a Sea-Bird Scientific SBE 911plus CTD equipped with duplicate temperature and conductivity sensors, a single pressure sensor, a Seapoint Chlorophyll *a* (Chl *a*) Fluorometer, a Sea-Bird WETLabs C-Star transmissometer, and a Sea-Bird SBE 43 dissolved oxygen sensor. Downcast data were binned at 1 m resolution following standard CalCOFI procedures (SIO-CalCOFI Technical Group 2017), and averages calculated from all profiles in each Cycle (Supporting Information Fig. S1). The depths of the chlorophyll maximum, particle maximum, thermocline, and 100 $\mu\text{m}/\text{kg}$ oxygen threshold were identified through visual examination of vertical profiles. The depth of the 1% light level was calculated from the in situ light attenuation coefficient (Beam *c*) and the depth of the buoyancy maximum was calculated from density and pressure using standard oceanographic equations in the R package “oce” (Kelley and Richards 2023).

Mesozooplankton collection and analysis

Zooplankton samples were collected, preserved, and analyzed by DNA sequencing and digital ZooScan imaging as described previously in Matthews et al. (2021). Briefly, at each location paired day and night depth-stratified 202 μm zooplankton net tows were conducted with a multiple opening/closing net and environmental sensing system (MOCNESS) between 0 and 400 m or 0 and 200 m over the continental shelf. Plankton samples were quantitatively split and preserved in 95% NH_4OH -buffered ethanol or 1.8% sodium borate-buffered formaldehyde.

Ethanol-preserved samples were split to 1/8th, DNA extracted in bulk, and each sample amplified in triplicate at the 18S-V4 (18S) and cytochrome oxidase I (COI) regions (Leray et al. 2013; Zhan et al. 2013). COI and 18S are the two most commonly used genes for metabarcoding (Bucklin et al. 2016). The high substitution rates of the protein-encoding COI mitochondrial gene allows for discrimination of closely related species. In contrast, the 18S nuclear gene is more conserved, allowing for detection of a wider range of taxonomic groups. Amplified sequences were processed in QIIME2 with *dada2* amplicon sequence variant (ASV) delimitation, followed by clustering into operational taxonomic units (OTUs) at 97% similarity at the COI marker (Callahan et al. 2016; Bolyen et al. 2018). COI amplicons were further filtered to remove sequences containing stop codons, in order to remove sequences resulting from pseudogenes, PCR errors, or sequencing error (Nugent et al. 2020). Resulting 18S ASVs and COI OTUs were given taxonomic assignments where possible based on the global MetaZooGene database for each marker, trimmed to the target region (Bucklin et al. 2021). Non-zooplankton taxa, including laboratory contaminants,

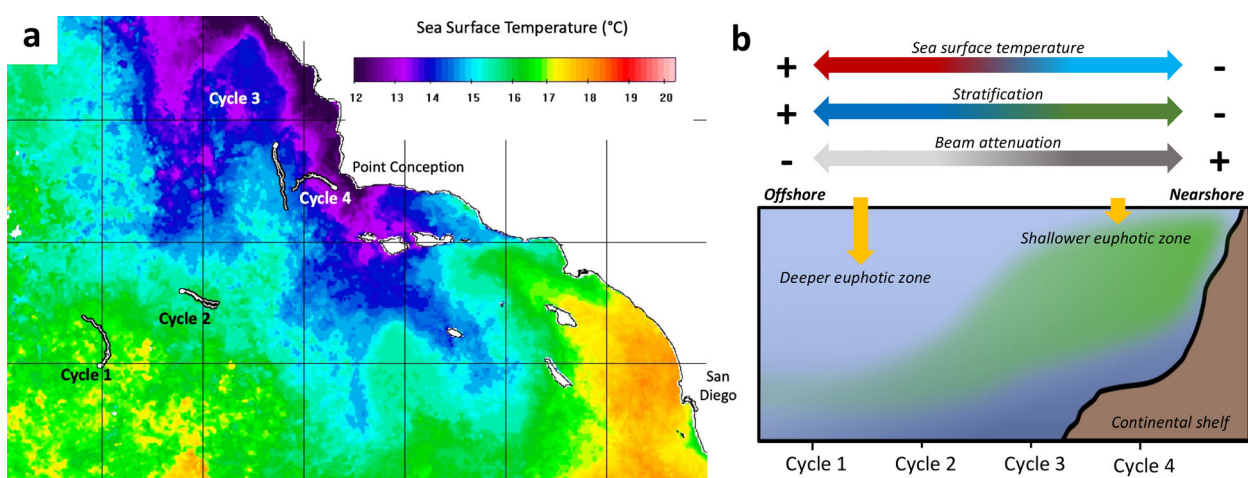


Fig. 1. (a) Sampling locations of four quasi-Lagrangian cycles within the CCE overlain on composite satellite sea surface temperature (SST), a proxy for stratification; and (b) a conceptual diagram of a cross-shore section of the water column showing gradients in stratification, SST, light attenuation (measured by beam attenuation), and Chl *a*. Satellite SST is a composite from 22 April to 11 May 2016. Each Cycle track shows the 3-day trajectory of the holey-sock drift array, around which day and night MOCNESS tows were centered. Zooplankton sampling was conducted between 0 and 400 m at Cycles 1–3 and 0–200 m at Cycle 4. Satellite image courtesy of M. Kahru, Scripps Institution of Oceanography.

all vertebrate sequences, and sequences unidentified at phylum level were removed, resulting in a dataset that included both holozooplankton and invertebrate meroplankton taxa (Supplementary Table S1a,b).

Formalin-preserved samples were imaged on a ZooScan (Gorsky et al. 2010) and sorted into 23 morphologically identifiable groups with a Convolutional Neural Network model, with all vignettes validated manually (Supplementary Table S2; Ellen et al. 2019). Carbon biomass was determined from length–carbon conversions, as in Lavaniegos and Ohman (2007).

Trait assignments

Each molecularly identified taxon was classified for the following traits: size, body composition, transparency, diet, feeding behavior, spawning strategy, presence of asexual reproduction, and diel vertical migration (DVM). The eight traits were selected to identify tradeoffs in ecological strategy, while targeting traits with sufficient data available for multiple taxonomic groups. Traits were assigned to taxa based on published trait databases (for copepods; Benedetti et al. 2016; Brun et al. 2017) and species-specific observations (Supplementary Table S3, Supplementary References).

Body size was selected as it is a “master trait” with significant impacts on predation risk and prey field, as well as metabolic rates and feeding needs (Litchman et al. 2013). Body size data were taxon-specific due to variability in taxonomic descriptions. For siphonophores, we used total colony length; for copepods, female prosome length; for euphausiids and amphipods, total length; and for medusae, bell height (if available) or bell width. Carbon content was included as a measure of gelatinous vs. non-gelatinous tissue composition, which is typically a tradeoff with size (Kiørboe 2013). Transparency was assigned as a qualitative category for each major taxonomic group, ranging from one (opaque) to five (transparent), based on mean transparency detected with transmitted red light using the Zooglider in situ imaging system (Ohman et al. 2019).

Two feeding variables were analyzed: trophic level (carnivore, omnivore, or herbivore) and feeding behavior (ambush, cruise, current, or parasitoid). Trophic level and feeding behavior followed previously published trait databases where available (Kiørboe 2011; Benedetti et al. 2016; Brun et al. 2016), supplemented with taxon-specific literature. Ambush feeding is characterized by lack of feeding movement prior to prey detection, including passive ambush (interception, as by pteropod mucous nets and ctenophore tentacles) and active ambush (pursuit of a prey item following detection, as displayed by chaetognaths and *Oithona* copepods). Cruise feeding refers to active movement of the predator through the water column with the intent to detect prey, such as visual predation by some heteropods, and mechanoreceptive detection of prey by *Clausocalanus* and *Metridia* copepods. Current feeding includes all taxa that set up feeding currents across a

portion of their body, such as feeding currents across mouth-parts or across tentacles. These currents can be for filter feeding (in ciliated taxa such as thaliaceans or pumping taxa such as appendicularians), direct interception (copepods), or scanning for individually handled prey (copepods). Finally, parasitoid feeding includes taxa identified as parasites or parasitoids, primarily amphipods. Trophic level and feeding behavior, and the modes we used for them, do not fully capture the range of feeding behaviors, mechanisms, and preferences found among zooplankton. However, we use them here because they are important measures of target prey field, trophic level, metabolic rate, and feeding effort, and are broadly comparable among zooplankton groups.

Spawning behavior (brooding or broadcast spawner) and evidence for asexual reproduction (whether obligate or alternating) were included as proxies for population turnover and the capacity of the population to exhibit bloom behavior. These reproductive traits are also related levels of parental investment in offspring and predation pressure (Carrier et al. 2018).

Finally, DVM behavior can have significant effects on food availability and predation risk, as well as the metabolic rate of the organism due to the costs of migration and temperature variability across depth. DVM behavior was based on observed day and night vertical distributions from sequence read abundance in our data. Taxa were classified as migratory if the modal depth of relative abundance shifted by at least two nets in at least one sampling location. After visual assessment of read distributions, DVM was only considered if a taxon was observed in at least two nets of each tow, if read differences were no more than twofold between day and night tows, and if the taxon comprised at least 0.01% of the total read abundance within all samples. These criteria are conservative and there may be additional migratory taxa we did not detect. However, the width of our sampling bins limits detection of small-amplitude vertical migrations. We refrain from assigning a behavior without strong evidence for it in the population we sampled, as our reads may represent any life history or developmental stage of the species and DVM behavior typically varies through the life history and may vary spatially.

Statistical analyses

Data analysis, statistical testing, and all visualizations were conducted in R version 4.2.1 (2022-2106-23), primarily with the packages *phyloseq*, *vegan*, and *tidyR*. To increase comparability among samples, we rarefied the dataset for each metabarcoding marker to the lowest sequencing depth observed in a biological sample, with rarefaction performed without replacement. Richness was calculated as the number of taxa present within each sample, after rarefaction. Non-metric dimensional scaling of Chao distance (Chao et al. 2005), which accounts for unseen species occurrences, was performed with the combined 18S and COI datasets after rarefaction. Mean depth of occurrence (MDO) was

calculated from the presence or absence in each depth stratum after filtering out occurrences that were < 5% of the total reads for the OTU or ASV. Cross-shore shifts in vertical distribution were defined as a change in MDO of at least 50 m, with vertical shifts tested between cycles independently for daytime and nighttime distributions, and only tested for the three cycles where sampling extended to 400 m. To account for taxa that were found only at two cycles, taxa were defined as exhibiting shifts if their MDO shifted deeper in the offshore direction between any two cycles. This allows for detection of vertical shifts even if a taxon was absent from or not detected in every Cycle. The linear relationship between OTU-specific MDO and environmental variables was tested independently for MDO calculated from 0 to 400 m for Cycles 1–3, and for MDO calculated from 0 to 200 m for all four cycles. Linear models for each environmental variable were compared using Aikake information criteria to identify the best-fit model. To examine vertical distributions of zooplankton traits, the total number of reads assigned to each trait state was summed, and total relative abundance of reads belonging to each trait state was treated as a single group (e.g., all reads belonging to taxa classified as herbivorous were summed, and the number of herbivorous reads was divided by the total number of reads classified as herbivorous, carnivorous, or omnivorous). Cross-shore shifts in single ASVs/OTUs or binary traits were not tested for statistical significance, due to low statistical power and absence of sampling replicates. All data processing and analysis scripts are available at <https://github.com/samatthews/VerticalHabitatShiftsCCE>.

Results

Cross-shore gradients in the zooplankton community

ZooScanning of zooplankton samples from four locations (“Cycles”) along a cross-shore gradient, sampled between the surface and 400 m, showed that non-eucalanid calanoid copepods (hereafter, “calanoids,” includes the order Calanoida except for the visually distinguishable family Eucalanidae) and eucalanid copepods (family Eucalanidae) dominated the overall zooplankton community, comprising 69% and 14% of the total zooplankton C biomass, respectively (Supplementary Table S2). At the 18S marker, 8.9 million reads were denoised into 1667 ASVs, and 8.3 million COI reads were clustered into 1282 OTUs at 97% similarity. Eighty percent of 18S ASVs and 40% of COI OTUs were identified at least to order, while only 34% and 26%, respectively, were identified to species (Table 1). Unidentified taxa were more common at COI than at 18S. Based on the best taxonomic identifications at 18S and COI, 27% and 16% of taxa were assigned trait values for size, 58% and 32% for diet, 65% and 33% for spawning behavior, 75% and 43% for asexual reproduction, 91% and 57% for carbon content, and 83% and 46% for transparency.

Table 1. Number of taxa with taxonomic identifications at each taxonomic rank, and number of taxa assigned a characteristic for each trait. Left column: 18S ASVs; right column: COI OTUs. DVM counts reflect the number of taxa exhibiting detectable DVM behavior within the present study.

	Number of taxa (18S ASVs)	Number of taxa (COI OTUs)
Assigned taxonomy		
Kingdom	1665	1282
Phylum	1534	741
Class	1485	596
Order	1334	519
Family	1031	402
Genus	802	352
Species	571	332
Assigned traits		
Maximum size	443	210
Diet	965	407
Feeding behavior	899	316
Spawning	1090	423
Asexual reproduction	1255	545
Carbon	1520	732
Transparency	1381	590
Exhibiting DVM	80	99
Total	1667	1282

DVM behavior was detected in 4.8% of 18S ASVs and 7.7% of COI OTUs.

Zooplankton richness within the study region was dominated by calanoid copepods, at both marker regions (828 taxa at 18S, 299 taxa at COI; Fig. 2b,d). Higher richness was also observed within Malacostraca and Hydrozoa (both markers), as well as Polychaeta and Thaliacea (18S). In the three cycles sampled to 400 m, total taxon richness decreased with depth both during the day and night, with the maximum in richness observed within the epipelagic zone (0–200 m) at all locations (Fig. 2). Within the epipelagic zone, the minimum in richness was observed near shore (Cycle 4, Fig. 2a,c). In the mesopelagic zone (200–400 m) richness was comparable among cycles and the minimum was observed in the offshore (Cycle 1, Fig. 2a,c).

We observed greater cross-shore differences in community composition within the epipelagic zone, with distinct epipelagic zooplankton communities at each cycle (Fig. 3, blue-green cool colors). In contrast, in the upper mesopelagic (200–400 m), community composition was more uniform across cycles (Fig. 3, yellow-red warm colors).

Copepods comprised the largest proportion of the zooplankton community, assessed via read abundance (Fig. 4). In addition, copepods were the most diverse taxon (Fig. 4a,c) and dominated carbon biomass (Supplementary Table S2). Within the copepod community, there were clear cross-shore changes

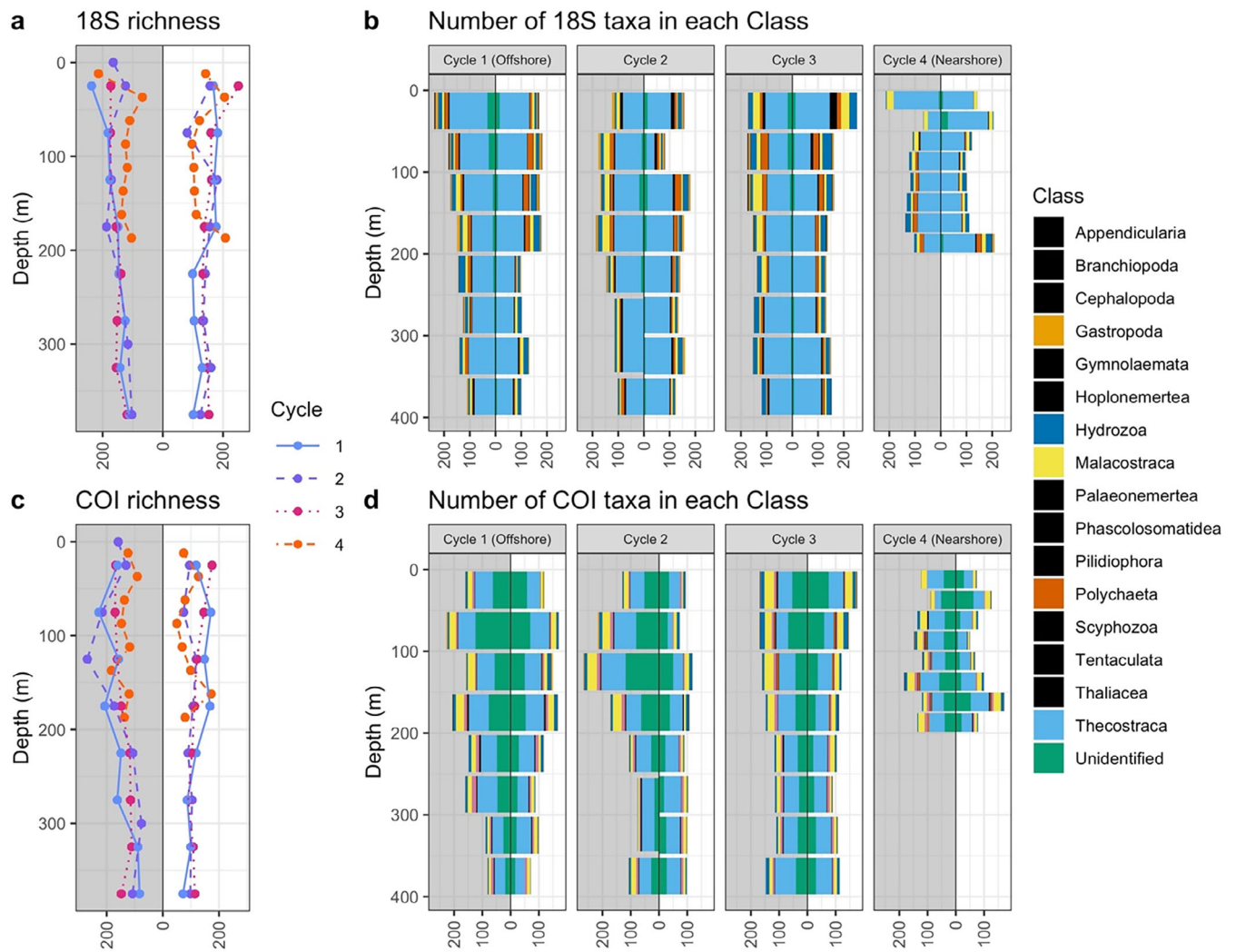


Fig. 2. Total richness (number of taxa observed within a sample) across depth for each cycle as detected (a) by the 18S marker and (c) by the COI marker; and the number of taxa identified as belonging to each taxonomic class (b) at the 18S marker and (d) by the COI marker. Colors in (a and c) indicate different sampling Cycles. Colors in (b and d) indicate taxon, with lower diversity taxa all shown in black. Within each Cycle, nighttime samples are shown on the shaded left panel, and daytime samples on the right.

in composition at the family level. Nearshore, the family Calanidae dominated the community, and while they remained present in the epipelagic zone, they became less abundant in the offshore. In the offshore the Clausocalanidae were relatively more important in the surface waters. The Eucalanidae were dominant at both markers and shifted to deeper waters offshore (Fig. 4b,d, Supporting Information Fig. S2). Carbon biomass of eucalanid copepods analyzed by ZooScan showed a similar pattern, confirming that relative read abundance for this dominant group reflected shifts in the biomass distribution of these animals (Supporting Information Fig. S2). The 18S marker detected higher abundances of Calanidae and Metridinidae. Euchaetidae were only detected at COI, and Oithonidae only at 18S (Fig. 4b,d). Despite these differences in taxonomic resolution, overall community-level

copepod richness and community composition showed similar patterns between markers.

Siphonophores exhibited distinct patterns in habitat partitioning among species from different suborders, which were taxonomically identified to species only at the COI marker. Siphonophore species in the suborder Calycophorae had restricted depth distributions, with vertical partitioning of the water column among species. Calycophorans (11 OTUs) exhibited a diverse assemblage with multiple species co-occurring in the epipelagic zone (*Amphicaryon acaule*, *Lensia campanella*, *L. conoidea*, and *Muggiaeaa atlantica*; Fig. 5a). In the mesopelagic zone, *Lensia achilles* was broadly distributed across all sampling locations and often occurred in the absence of other species. The calycophoran assemblage also exhibited a cross-shore shift in vertical habitat. Most species

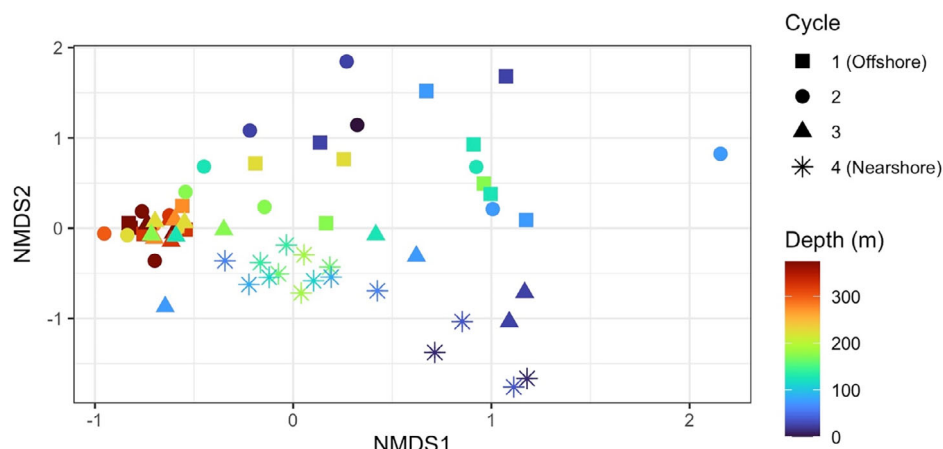


Fig. 3. Non-metric multidimensional scaling ordination of Chao distance among samples. Shapes denote the sampling location ('cycle'), colors indicate the midpoint of the sampling depth.

moved deeper offshore, and the vertical richness maximum shifted into the upper mesopelagic zone offshore. In comparison, physonect siphonophores exhibited lower overall richness (five OTUs). Physonect siphonophores had restricted or patchy distributions with no clear vertical habitat partitioning among species, and no cross-shore shifts in vertical distributions (Fig. 5b).

Euphausiid biomass was highest nearshore, and euphausiid distributions shifted deeper in the water column with distance offshore, as detected by both ZooScan biomass and metabarcoding reads (Fig. 6). Euphausiid reads were identified to species only at the COI marker, but the most abundant Euphausiidae ASVs in the 18S dataset exhibit similar patterns to the identified species at the COI marker (Supporting Information Fig. S3). In addition to cross-shore changes in the vertical distributions of individual species (primarily *Euphausia pacifica* and *Hansarsia difficilis*), there were cross-shore and vertical changes in euphausiid species composition. The euphausiid community in the upwelling region (Cycles 3–4) was dominated by *Euphausia pacifica*, which was also observed offshore in lower relative abundances and deeper waters. *Hansarsia difficilis* was broadly distributed across the region, but deeper in the water column than *E. pacifica*. *Nyctiphanes simplex* was restricted to the nearshore, while *Thysanoessa gregaria* was observed primarily in Cycle 2 and the deeper-dwelling *Thysanopoda acutifrons* was almost entirely restricted to Cycle 1. In total, the euphausiid community composition showed cross-shore changes in species composition in addition to the family level shift to deeper waters in the offshore region (Fig. 6).

In total, cross-shore shifts in vertical distributions of zooplankton taxa across Cycles 1–3 were detectable in 161 ASVs at 18S (10%), and 165 OTUs at COI (13%). Within these vertically shifting taxa, 9 and 11 (5.6% and 6.6% respectively) exhibited vertical shifts both day and night. Of taxa observed in all three cycles, 65.4% and 73.3% of ASVs and OTUs exhibited vertical shifts in MDO, while only 30% and 34% of taxa observed in two cycles exhibited vertical shifts. Compared

to the overall percentage of taxa exhibiting vertical shifts, vertical shifts were overrepresented within Calanoida, Euphausiacea, Trachymedusae, Ctenophora, and Mollusca ($> 1.5 \times$ the average of all taxa; Supplementary Table S4). Comparison of linear models found that vertical shifts were best explained by the depth of the 1% light level (COI data) and the depth of the chlorophyll maximum (18S data; Supplementary Table S5).

Zooplankton traits

We observed predictable cross-shore changes in the trait composition of the zooplankton community for three of the eight traits analyzed (Fig. 7). Brooding behavior was lowest nearshore, with a monotonic increase in brooding behavior with distance offshore (Fig. 7a). Current feeding was the most common feeding mode in all four cycles, but offshore there was a slight increase in cruise feeding and ambush feeding (Fig. 7b). Dietary modes also became more heterogeneous offshore, with increased contributions from carnivores and herbivores and decreasing proportions of omnivores (Fig. 7c). We did not detect cohesive changes in zooplankton community composition for five of the eight traits: asexual reproduction, DVM behavior, body size, transparency, and body carbon composition (Supporting Information Fig. S4). Traits without clear monotonic trends included traits with poorly resolved trait data (e.g., body carbon composition, body size) and traits that were exhibited by taxa with marker-specific amplification or identification biases (e.g., asexual reproduction, DVM behavior).

To identify which zooplankton traits influence vertical habitat use, we tested whether the vertical distributions of species traits changed in the cross-shore direction. We found the strongest differences among diets (Fig. 8). Carnivorous zooplankton exhibited strong cross-shore deepening in vertical distribution, especially at night, while the peak in herbivore read abundance remained in the epipelagic zone both day and night across all four cycles (Fig. 8). Carnivores (296 18S ASVs,

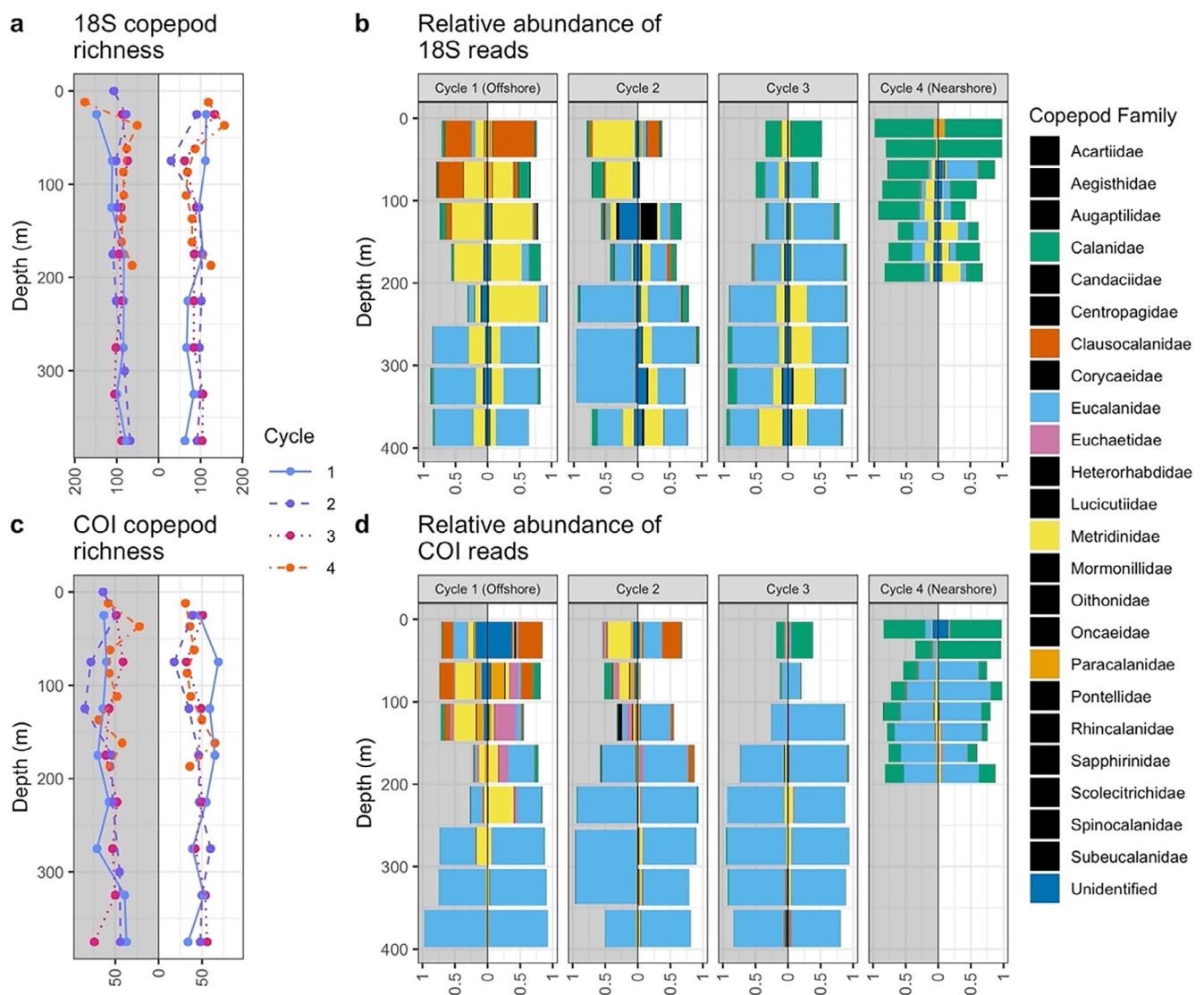


Fig. 4. Total copepod richness detected (a) by 18S, and (b) by COI, and the relative abundance of each copepod family as a proportion of the total zooplankton community for (b) the 18S community and (d) the COI community. Colors in (a and c) indicate different sampling cycles. Colors in (b and d) indicate taxon, with rare copepod families all shown in black. Within cycles, nighttime samples are shown on the shaded left panel, and daytime samples on the right.

207 COI OTUs) were dominated by copepods, hydrozoans, polychaetes, and eucardid and peracardid malacostracans. Herbivorous taxa (387 18S OTUs, 62 COI OTUs) were primarily calanoid copepods (Supplementary Tables S6, S7). Omnivores were broadly distributed throughout the water column and across Cycles, but thaliacean omnivores exhibited herbivore-like distributions primarily restricted to the epipelagic zone (Supporting Information Fig. S5).

Discussion

Using a SFTS, we assessed whether zooplankton community composition and vertical habitat use changes predictably

with ocean stratification. A trait-based analysis of metabarcoding sequences from two marker regions, complemented by digital imaging with a ZooScan, revealed clear cross-shore trends in both community composition and zooplankton vertical habitat use. Our study area extended from the nearshore active upwelling ecosystem, across the California Current, to offshore stratified mesotrophic waters (see schematic diagram in Fig. 1b). Across the gradient in stratification, shifts in vertical habitat use were exhibited by individual ASVs and OTUs as well as across the full zooplankton community, with deeper distributions in the offshore region. Vertical shifts varied among organisms with different diet modes, and there were cross-shore changes in reproductive strategy, feeding behavior, and dietary strategy.

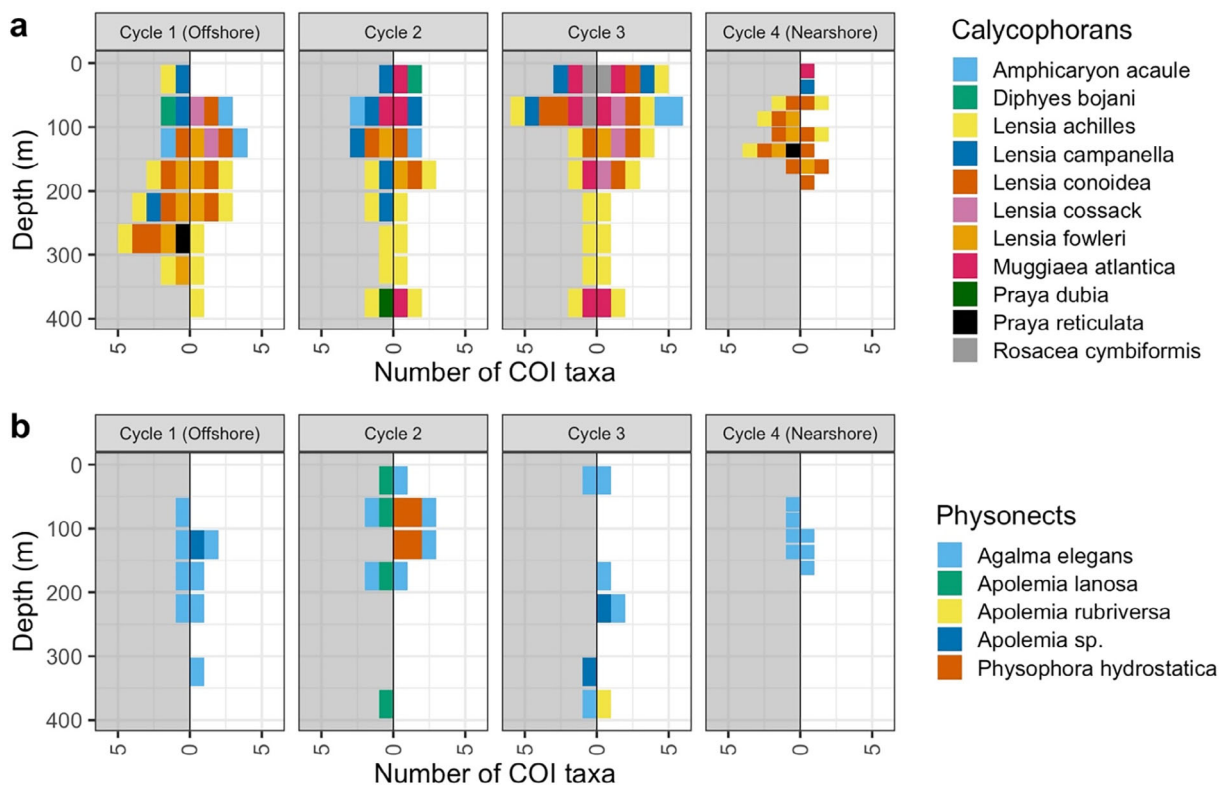


Fig. 5. Observed richness of siphonophore taxa at the COI marker region (a) within the calycophoran group and (b) within the physonect group. Colors indicate taxon. Within each cycle, nighttime samples are shown on the gray-shaded left panel, and daytime samples on the right.

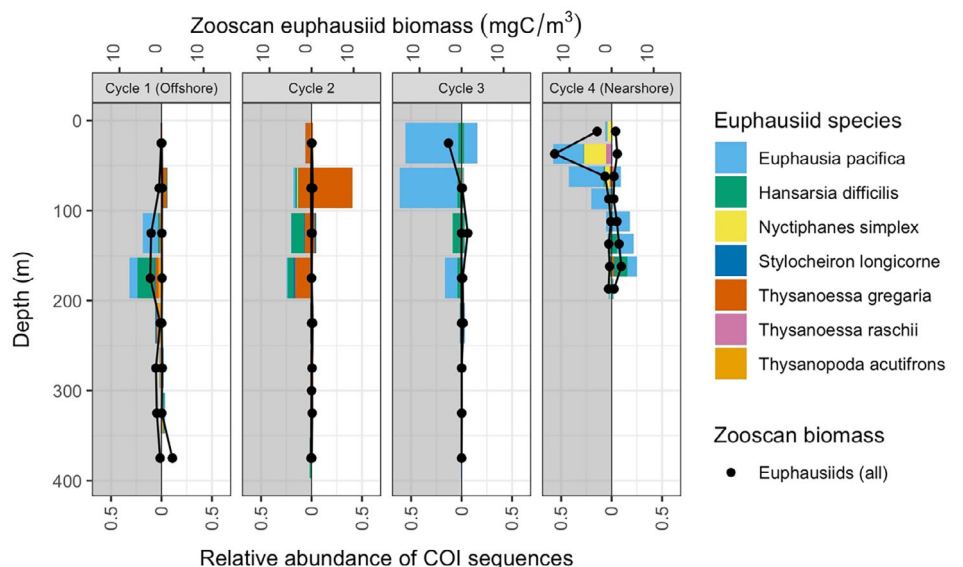


Fig. 6. Relative read abundance of all euphausiid taxa detected by COI (colored bars), as well as total euphausiid biomass from digital ZooScan imaging (black points). Colors represent taxa. Within cycles, nighttime samples are shown on the shaded left panel, and daytime samples on the right.

As discussed below, species traits are key to understanding the ecological relationship between zooplankton and their environment, as well as to predicting potential effects of ocean changes on zooplankton communities.

Changes in zooplankton species

We observed comparable levels of species richness at 18S and COI, with both communities dominated by calanoid copepods. Previous metabarcoding analyses of metazoans in

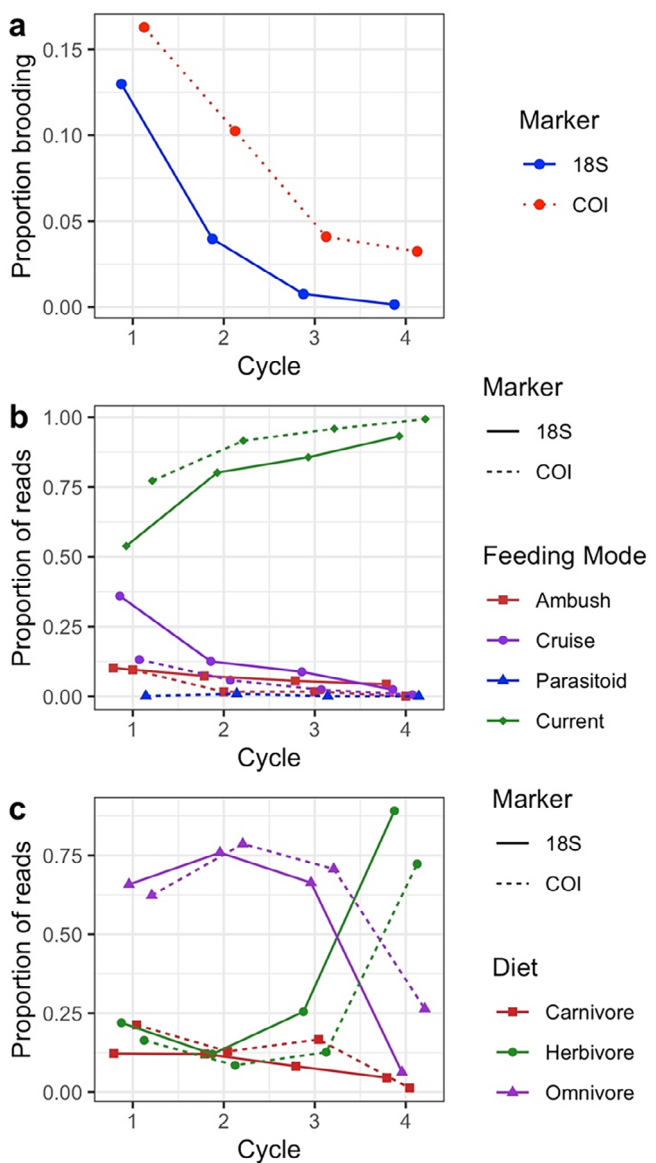


Fig. 7. Proportions of zooplankton reads that were identified as taxa (a) with brooding behavior of embryos or juveniles; (b) primarily exhibiting each feeding strategy; and (c) primarily belonging to each dietary group.

the CCE have reported taxon richness ranging from 21% to 2700% of the richness observed in the current study (342 to 44,837 at 18S and 1596 to 21,402 at COI; Pitz et al. 2020), likely due to bioinformatic differences. The dominance of copepods, malacostracans, cnidarians, and thaliaceans in our study, both in richness and abundance, is a slight departure from previous, morphologically determined records of community composition. Over a 56-year time series, Lavaniegos and Ohman (2007) observed consistent dominance of copepods, malacostracans, chaetognaths and tunicates, but not cnidarians. The richness of cnidarians in our study reflects the ability to easily differentiate small, hard to identify specimens

through genetic sequencing, as well as the finer mesh size we used (202 μm rather than 505 μm). We were not able to identify most cnidarian sequences to species, indicating a need for additional reference specimen sequencing, as well as morphological and ecological studies on this group.

Although some metabarcoding studies on metazoan zooplankton have been published for the region (Pitz et al. 2020), vertical zooplankton species richness patterns appear not to have been previously documented within the CCE. We observed the highest richness within the epipelagic zone, with the depth of the richness maximum varying between the surface and 150 m, depending on the marker and sampling location. Within copepods and siphonophores, we also observed higher richness in the epipelagic than in the mesopelagic zone. Previous work in other systems has found the zooplankton richness maximum in the epipelagic (tropical Eastern Pacific, ~50 m), upper mesopelagic (North Pacific Subtropical Gyre, ~400–600 m), and lower mesopelagic (Arctic Basin, 500–1000 m; Longhurst 1985; Kosobokova and Hopcroft 2010; Sommer et al. 2017). These systems range from stable, stratified, oligotrophic gyre systems (Eastern Pacific) to highly seasonal polar systems (Arctic Basin). Across these distinct ecosystems, richness maxima appear to be generally associated with thermoclines. In contrast, the richness maxima across our Cycles were not associated with the depth of the thermocline, despite both consistently occurring within the epipelagic zone. Our results suggest scale-dependence of this association between richness maxima and the physical environment.

The vertical distribution of many individual OTUs, some complete groups, and the overall zooplankton community shifted to deeper depths in clearer, more stratified offshore waters. Within copepods, similar vertical changes have previously been observed in adult females of *Pleuromamma* species, with vertical distributions in the Northeast Pacific shifting to deeper depths in the offshore (Haury 1988). Euphausiid species are closely associated with water masses, and the shifting community composition we observed in the hydrographically complex southern California Current likely reflects the vertical and horizontal water mass structure of the region (Lilly and Ohman 2018). Cross-shore shifts in community composition are well documented within the CCE, but species-specific changes in vertical habitat have not previously been reported in the southern CCE. Across the gradient in water column stratification, the association between vertical distributions and light attenuation (or optical environment) suggests that many zooplankton taxa can select their preferred vertical habitat within the water column. Vertical shifts may minimize the range of environments the taxon is exposed to throughout its biogeographic range, or may even allow taxa to maintain a constant ambient environment. We also observed larger horizontal distributions among taxa with vertically shifting distributions, indicating that active vertical habitat selection can increase the biogeographic range of a species. Our results

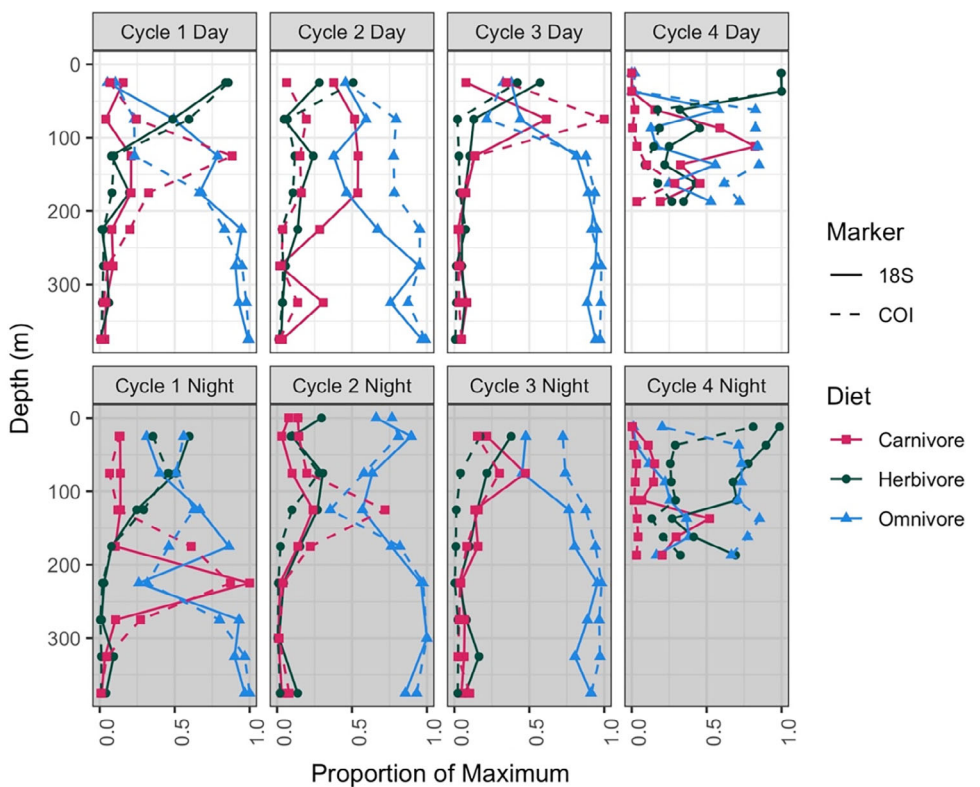


Fig. 8. Vertical distribution of dietary traits at each cycle. Upper row: daytime (white background), lower row: nighttime (gray background). Relative abundance of COI and 18S reads assigned to each dietary characteristic is scaled relative to the maximum abundance for the characteristic (carnivores in red; herbivores in green, and omnivores in purple).

indicate that the vertical shifts previously described across the CCE (Ohman and Romagnan 2016) are comprised both of changes in species composition and changes in vertical habitat use by more broadly distributed species.

Changes in zooplankton traits

Across the gradient in stratification, we observed predictable, directional changes in the trait composition of the zooplankton community for brooding behavior, feeding strategy, and dietary mode. Brooding behavior increased with distance offshore, detected by both molecular marker regions. Taxa with the potential for asexual reproduction showed a tendency toward higher prevalence offshore (Cycles 1 and 3), and lower prevalence nearshore. Together, these results suggest that reproductive strategies in productive upwelling waters tend toward production of large numbers of energetically inexpensive larvae. In these relatively opaque coastal waters, food availability for predators is high and the individual predation risk of unprotected larvae is lower (Folt and Burns 1999). Offshore, brooding behavior becomes more common, reflecting increased parental investment, likely due to greater visual predation risk to vulnerable larvae and juveniles as well as lower probability of mate encounter.

Offshore, feeding behavior became more heterogeneous, with cruise and ambush comprising 24–48% of feeding modes offshore of the California current. Increased diversity of feeding modes suggests increasing trophic complexity of the zooplankton community in the food-depleted stratified waters offshore (Takimoto and Post 2013). Carnivory increased in the offshore as well, with marker-specific differences in herbivory and omnivory due to muted amplification of herbivorous calanoids at the COI marker. Zooplankton feeding modes and diet have previously been identified as key traits that may influence the effects of community change on ecosystem function (Saint-Béat et al. 2022). Our analysis indicates that current feeders are sensitive to ocean stratification, but that carnivores actively shift their vertical distributions and become relatively more abundant in the stratified offshore region of the CCE.

Vertical habitat use varied among dietary strategies, with stronger vertical migrations for carnivores than for herbivores, as well increases in the dominance of carnivory and herbivory in offshore stratified waters. While some zooplankton exhibit visual acuity (e.g., heteropods, some pontellid copepods), vision is typically restricted to detection of light and movement (Kiørboe 2011) and prey detection largely depends on mechanosensory or chemosensory reception rather than vision

(Martens et al. 2015). We did not observe differences in cross-shore vertical habitat among feeding modes, indicating that changes in prey detection potential is unlikely to drive the response of carnivorous taxa to the optical environment. However, many zooplankton taxa in our dataset are preyed upon by adult and larval fish, and the distributions of many larval fishes closely track the optical environment (Job and Bellwood 2000). It is possible that zooplankton are driven deeper in clearer waters due to predation risk from visual predators, and deeper distributions of carnivorous zooplankton are due to non-visual carnivores following potential prey into deeper waters. Herbivores appear to be associated with their food source, with vertical distributions associated with the chlorophyll maximum or associated marine snow (e.g., Whitmore and Ohman 2021). Examination of thaliaceans, detected only by 18S, indicates that the three feeding modes we assigned may insufficiently describe some taxa. We classified thaliaceans as omnivores (Bone 1998), although vertical distributions of thaliaceans were primarily restricted to the upper epipelagic zone, most similar to herbivores (Supporting Information Fig. S5). Future analyses could investigate whether thaliaceans in the CCE primarily function as herbivores.

In contrast, the prevalence of asexual reproduction, DVM behavior, maximum body size, transparency, and body carbon composition were not predictable. We observed a slight increase in DVM in the offshore stratified waters. Nearshore, proportions of the community with DVM behavior differed between the 18S and COI resolved communities. These differences are primarily due to lower relative abundances of calanoid copepods in the COI-resolved community, which reduced detection of DVM. Asexual reproduction peaked overall at an intermediate offshore location, which may reflect a community adapted to respond rapidly to transient pulses in food availability due to intermittent upwelling and horizontal transport of chlorophyll-rich coastal waters (Chabert et al. 2021).

Overall, comparisons among the eight traits assessed across two metabarcoding datasets showed differential vertical habitat use among zooplankton with different diets. We detected cross-shore shifts toward an offshore community with more heterogeneous feeding strategies and increased parental investment. Feeding (or growth), survival, and reproduction are the three fundamental activities each organism must accomplish (Litchman et al. 2013), and our results highlight the impact of changing ocean environments on all three mandates. Vertical habitat use is influenced by ocean stratification, but differential responses between trophic groups reflect differences in prey availability. In more nutrient limited transition and offshore waters, reproductive strategies shift, with increased brooding reflecting greater parental investment and decreased rates of mate encounter.

The SFTS

Space for time substitution assumes that the principal forcing mechanisms are similar in space and time. In our study

region, the cross-shore changes in density stratification reported here parallel documented temporal increases in water column stratification for the same region (e.g., Lavaniegos and Ohman 2007; Xiu et al. 2018). Such changes in stratification in the CCE region are associated with alterations to nutrient supply (Aksnes et al. 2007), concentrations of phytoplankton, and optical transparency of the water column (Aksnes and Ohman 2009; Ohman and Romagnan 2016), all of which are factors that directly or indirectly influence zooplankton growth and survivorship. Hence, there is parallelism of the underlying forcing mechanisms. Although subregions of a dynamic upwelling region are unlikely to be at steady-state, the kind of broader cross-shore changes in density stratification that we analyze here are persistent features that can nearly always be found. Where SFTS is less likely to be useful is when environmental conditions cross a threshold or “tipping point” (sensu Scheffer et al. 2009) that have not been sampled in a spatial survey, leading to new functional relationships (Lovell et al. 2023). It is not clear when or whether such tipping points will be crossed in the present study region, but in the interim, the SFTS hypothesis provides one of the few tools available to forecast future ecosystem states based on empirical measurements.

Future priorities

Using a space-for-time framework, we used changes in zooplankton communities along an environmental gradient ranging from active upwelling to more stratified mesotrophic habitats to predict effects of ocean warming and increased stratification on zooplankton communities in a major coastal upwelling biome. For some major zooplankton traits, we did not find predictable changes, perhaps due to limitations in taxonomic or trait assignments. Reference databases for assigning taxonomic identities to metabarcoding sequences need to be greatly expanded in order to link molecular data with the wealth of ecological observations that exist for many species. Similarly, a comprehensive zooplankton traits database encompassing multiple taxa would facilitate the identification of trait interactions and ecological tradeoffs among zooplankton functional groups, enabling better predictions of zooplankton responses to a changing ocean.

Our study suggests that increased ocean stratification will restructure zooplankton community composition and habitat use. Zooplankton in a future, more stratified CCE will exhibit increased rates of carnivory, cruise feeding, and brooding of offspring. Carnivores will likely shift their vertical distributions most in response to ocean warming and stratification. Increased ocean stratification may lead to a zooplankton community that dwells deeper in the water column, with increased carnivory, more heterogeneous feeding strategies, and greater parental investment. The observed changes are expected to be concentrated in the epipelagic ocean, but extend into the upper mesopelagic.

Data availability statement

ZooScan data are available through CCE-LTER DataZoo. Raw 18S and COI sequences are under NCBI SRA PR-JNA679794. Code, ZooScan data, CTD data, and sample metadata is available at <https://github.com/samatthews/VerticalHabitatShiftsCCE>.

References

- Aksnes, D. L., M. D. Ohman, and P. Rivière. 2007. Optical effect on the nitracline in a coastal upwelling area. *Limnol. Oceanogr.* **52**: 1179–1187. doi:[10.4319/lo.2007.52.3.1179](https://doi.org/10.4319/lo.2007.52.3.1179)
- Aksnes, D. L., and M. D. Ohman. 2009. Multi-decadal shoaling of the euphotic zone in the southern sector of the California current system. *Limnol. Oceanogr.* **54**: 1272–1281. doi:[10.4319/lo.2009.54.4.1272](https://doi.org/10.4319/lo.2009.54.4.1272)
- Benedetti, F., S. Gasparini, and S.-D. Ayata. 2016. Identifying copepod functional groups from species functional traits. *J. Plankton Res.* **38**: 159–166. doi:[10.1093/plankt/fbv096](https://doi.org/10.1093/plankt/fbv096)
- Benedetti, F., J. Wydler, and M. Vogt. 2022. Copepod functional traits and groups show divergent biogeographies in the global ocean. *J. Biogeogr.* **50**: 8–22. doi:[10.1111/jbi.14512](https://doi.org/10.1111/jbi.14512)
- Bograd, S. J., I. D. Schroeder, and M. G. Jacox. 2019. A water mass history of the Southern California current system. *Geophys. Res. Lett.* **46**: 6690–6698. doi:[10.1029/2019GL082685](https://doi.org/10.1029/2019GL082685)
- Bolyen, E., and others. 2018. QIIME 2: Reproducible, interactive, scalable, and extensible microbiome data science. *PeerJ Preprints* **6**: e27295v2.
- Bone, Q. 1998. The biology of pelagic tunicates. Oxford Univ. Press.
- Brun, P., M. R. Payne, and T. Kiørboe. 2016. Trait biogeography of marine copepods—an analysis across scales. *Ecol. Lett.* **19**: 1403–1413. doi:[10.1111/ele.12688](https://doi.org/10.1111/ele.12688)
- Brun, P., M. R. Payne, and T. Kiørboe. 2017. A trait database for marine copepods. *Earth Syst. Sci. Data* **9**: 99–113. doi:[10.1594/PANGAEA.862968](https://doi.org/10.1594/PANGAEA.862968)
- Bucklin, A., P. K. Lindeque, N. Rodriguez-Ezpeleta, A. Albaina, and M. Lehtiniemi. 2016. Metabarcoding of marine zooplankton: Prospects, progress and pitfalls. *J. Plankton Res.* **38**: 393–400. doi:[10.1093/plankt/fbw023](https://doi.org/10.1093/plankt/fbw023)
- Bucklin, A., and others. 2021. Toward a global reference database of COI barcodes for marine zooplankton. *Mar. Biol.* **168**: 78. doi:[10.1007/s00227-021-03887-y](https://doi.org/10.1007/s00227-021-03887-y)
- Callahan, B. J., P. J. McMurdie, M. J. Rosen, A. W. Han, A. J. A. Johnson, and S. P. Holmes. 2016. DADA2: High-resolution sample inference from Illumina amplicon data. *Nat. Methods* **13**: 581–583. doi:[10.1038/nmeth.3869](https://doi.org/10.1038/nmeth.3869)
- Capotondi, A., M. A. Alexander, N. A. Bond, E. N. Curchitser, and J. D. Scott. 2012. Enhanced upper ocean stratification with climate change in the CMIP3 models. *J. Geophys. Res. Oceans* **117**. doi:[10.1029/2011JC007409](https://doi.org/10.1029/2011JC007409)
- Carrier, T. J., A. M. Reitzel, and A. Heyland. 2018. Evolutionary ecology of marine invertebrate larvae. Oxford Univ. Press.
- Chabert, P., F. D'ovidio, V. Echevin, M. R. Stukel, and M. D. Ohman. 2021. Cross-shore flow and implications for carbon export in the California current ecosystem: A Lagrangian analysis. *J. Geophys. Res. Oceans* **126**: e2020JC016611. doi:[10.1029/2020JC016611](https://doi.org/10.1029/2020JC016611)
- Chao, A., R. L. Chazdon, R. K. Colwell, and T.-J. Shen. 2005. A new statistical approach for assessing similarity of species composition with incidence and abundance data. *Ecol. Lett.* **8**: 148–159. doi:[10.1111/j.1461-0248.2004.00707.x](https://doi.org/10.1111/j.1461-0248.2004.00707.x)
- Damgaard, C. 2019. A critique of the space-for-time substitution practice in community ecology. *Trends Ecol. Evol.* **34**: 416–421. doi:[10.1016/j.tree.2019.01.013](https://doi.org/10.1016/j.tree.2019.01.013)
- Ellen, J. S., C. A. Graff, and M. D. Ohman. 2019. Improving plankton image classification using context metadata. *Limnol. Oceanogr. Methods* **17**: 439–461. doi:[10.1002/lom3.10324](https://doi.org/10.1002/lom3.10324)
- Evans, L. E., A. G. Hirst, P. Kratina, and G. Beaugrand. 2020. Temperature-mediated changes in zooplankton body size: Large scale temporal and spatial analysis. *Ecography* **43**: 581–590. doi:[10.1111/ecog.04631](https://doi.org/10.1111/ecog.04631)
- Folt, C. L., and C. W. Burns. 1999. Biological drivers of zooplankton patchiness. *Trends Ecol. Evol.* **14**: 300–305. doi:[10.1016/S0169-5347\(99\)01616-X](https://doi.org/10.1016/S0169-5347(99)01616-X)
- Gorsky, G., and others. 2010. Digital zooplankton image analysis using the ZooScan integrated system. *J. Plankton Res.* **32**: 285–303. doi:[10.1093/plankt/fbp124](https://doi.org/10.1093/plankt/fbp124)
- Haury, L. R. 1988. Vertical distribution of Pleuromamma (Copepoda: Metridinidae) across the eastern North Pacific Ocean. *Hydrobiologia* **167**: 335–342.
- Heneghan, R. F., and others. 2020. A functional size-spectrum model of the global marine ecosystem that resolves zooplankton composition. *Ecol. Model.* **435**: 109265. doi:[10.1016/j.ecolmodel.2020.109265](https://doi.org/10.1016/j.ecolmodel.2020.109265)
- Job, S. D., and D. R. Bellwood. 2000. Light sensitivity in larval fishes: Implications for vertical zonation in the pelagic zone. *Limnol. Oceanogr.* **45**: 362–371. doi:[10.4319/lo.2000.45.2.0362](https://doi.org/10.4319/lo.2000.45.2.0362)
- Kahru, M., Z. Lee, R. M. Kudela, M. Manzano-Sarabia, and B. Greg Mitchell. 2015. Multi-satellite time series of inherent optical properties in the California current. *Deep Sea Res. II Top. Stud. Oceanogr.* **112**: 91–106. doi:[10.1016/j.dsr2.2013.07.023](https://doi.org/10.1016/j.dsr2.2013.07.023)
- Kelley, D., and C. Richards. 2023. oce: Analysis of oceanographic data. *oce*.
- Kiørboe, T. 2011. How zooplankton feed: Mechanisms, traits and trade-offs. *Biol. Rev.* **86**: 311–339. doi:[10.1111/j.1469-185X.2010.00148.x](https://doi.org/10.1111/j.1469-185X.2010.00148.x)
- Kiørboe, T. 2013. Zooplankton body composition. *Limnol. Oceanogr.* **58**: 1843–1850. doi:[10.4319/lo.2013.58.5.1843](https://doi.org/10.4319/lo.2013.58.5.1843)
- Kosobokova, K. N., and R. R. Hopcroft. 2010. Diversity and vertical distribution of mesozooplankton in the Arctic's

- Canada Basin. Deep Sea Res. II Top. Stud. Oceanogr. **57**: 96–110. doi:[10.1016/j.dsr2.2009.08.009](https://doi.org/10.1016/j.dsr2.2009.08.009)
- Landry, M. R., M. D. Ohman, R. Goericke, M. R. Stukel, and K. Tsyrklevich. 2009. Lagrangian studies of phytoplankton growth and grazing relationships in a coastal upwelling ecosystem off Southern California. Prog. Oceanogr. **83**: 208–216. doi:[10.1016/j.pocean.2009.07.026](https://doi.org/10.1016/j.pocean.2009.07.026)
- Lavaniegos, B. E., and M. D. Ohman. 2007. Coherence of long-term variations of zooplankton in two sectors of the California current system. Prog. Oceanogr. **75**: 42–69. doi:[10.1016/j.pocean.2007.07.002](https://doi.org/10.1016/j.pocean.2007.07.002)
- Leray, M., J. Y. Yang, C. P. Meyer, S. C. Mills, N. Agudelo, V. Ranwez, J. T. Boehm, and R. J. Machida. 2013. A new versatile primer set targeting a short fragment of the mitochondrial COI region for metabarcoding metazoan diversity: Application for characterizing coral reef fish gut contents. Front. Zool. **10**: 34. doi:[10.1186/1742-9994-10-34](https://doi.org/10.1186/1742-9994-10-34)
- Li, G., L. Cheng, J. Zhu, K. E. Trenberth, M. E. Mann, and J. P. Abraham. 2020. Increasing ocean stratification over the past half-century. Nat. Clim. Chang. **10**: 1116–1123. doi:[10.1038/s41558-020-00918-2](https://doi.org/10.1038/s41558-020-00918-2)
- Lilly, L. E., and M. D. Ohman. 2018. CCE IV: El Niño-related zooplankton variability in the southern California current system. Deep Sea Res. I Oceanogr. Res. Pap. **140**: 36–51. doi:[10.1016/j.dsr.2018.07.015](https://doi.org/10.1016/j.dsr.2018.07.015)
- Litchman, E., M. D. Ohman, and T. Kiørboe. 2013. Trait-based approaches to zooplankton communities. J. Plankton Res. **35**: 473–484. doi:[10.1093/plankt/fbt019](https://doi.org/10.1093/plankt/fbt019)
- Longhurst, A. R. 1985. Relationship between diversity and the vertical structure of the upper ocean. Deep Sea Res. Part A Oceanog. Res. Pap. **32**: 1535–1570. doi:[10.1016/0198-0149\(85\)90102-5](https://doi.org/10.1016/0198-0149(85)90102-5)
- Lovell, R. S. L., S. Collins, S. H. Martin, A. L. Pigot, and A. B. Phillipmore. 2023. Space-for-time substitutions in climate change ecology and evolution. Biol. Rev. doi:[10.1111/brv.13004](https://doi.org/10.1111/brv.13004)
- Lynn, R. J., and J. J. Simpson. 1987. The California current system: The seasonal variability of its physical characteristics. J. Geophys. Res. Oceans **92**: 12947–12966. doi:[10.1029/JC092iC12p12947](https://doi.org/10.1029/JC092iC12p12947)
- Martens, E. A., N. Wadhwa, N. S. Jacobsen, C. Lindemann, K. H. Andersen, and A. Visser. 2015. Size structures sensory hierarchy in ocean life. Proc. Roy. Soc. B: Biol. Sci. **282**: 20151346. doi:[10.1098/rspb.2015.1346](https://doi.org/10.1098/rspb.2015.1346)
- Martini, S., and others. 2021. Functional trait-based approaches as a common framework for aquatic ecologists. Limnol. Oceanogr. **66**: 965–994. doi:[10.1002/lno.11655](https://doi.org/10.1002/lno.11655)
- Matthews, S., E. Goetze, and M. D. Ohman. 2021. Recommendations for interpreting zooplankton metabarcoding and integrating molecular methods with morphological analyses. ICES J. Mar. Sci. **78**: 3387–3396. doi:[10.1093/icesjms/fsab107](https://doi.org/10.1093/icesjms/fsab107)
- Morrow, R. M., M. D. Ohman, R. Goericke, T. B. Kelly, B. M. Stephens, and M. R. Stukel. 2018. CCE V: Primary production, mesozooplankton grazing, and the biological pump in the California current ecosystem: Variability and response to El Niño. Deep Sea Res. I Oceanogr. Res. Pap. **140**: 52–62. doi:[10.1016/j.dsr.2018.07.012](https://doi.org/10.1016/j.dsr.2018.07.012)
- Nugent, C. M., T. A. Elliott, S. Ratnasingham, and S. J. Adamowicz. 2020. Coil: An R package for cytochrome *c* oxidase I (COI) DNA barcode data cleaning, translation, and error evaluation. Genome **63**: 291–305. doi:[10.1139/gen-2019-0206](https://doi.org/10.1139/gen-2019-0206)
- Ohman, M., K. Barbeau, P. Franks, R. Goericke, M. Landry, and A. Miller. 2013. Ecological transitions in a coastal upwelling ecosystem. Oceanography **26**: 210–219.
- Ohman, M. D., J. R. Powell, M. Picheral, and D. W. Jensen. 2012. Mesozooplankton and particulate matter responses to a deep-water frontal system in the southern California current system. J. Plankton Res. **34**: 815–827. doi:[10.1093/plankt/fbs028](https://doi.org/10.1093/plankt/fbs028)
- Ohman, M. D., and J.-B. Romagnan. 2016. Nonlinear effects of body size and optical attenuation on diel vertical migration by zooplankton: Body size- and light-dependent DVM. Limnol. Oceanogr. **61**: 765–770. doi:[10.1002/lno.10251](https://doi.org/10.1002/lno.10251)
- Ohman, M. D., R. E. Davis, J. T. Sherman, K. R. Grindley, B. M. Whitmore, C. F. Nickels, and J. S. Ellen. 2019. Zooglider: An autonomous vehicle for optical and acoustic sensing of zooplankton. Limnol. Oceanogr. Methods **17**: 69–86. doi:[10.1002/lom3.10301](https://doi.org/10.1002/lom3.10301)
- Peijnenburg, K. T. C. A., and E. Goetze. 2013. High evolutionary potential of marine zooplankton. Ecol. Evol. **3**: 2765–2781. doi:[10.1002/ece3.644](https://doi.org/10.1002/ece3.644)
- Pickett, S. T. A. 1989. Space-for-time substitution as an alternative to long-term studies, p. 110–135. In G. E. Likens [ed.], Long-term studies in ecology: Approaches and alternatives. Springer.
- Pitz, K. J., J. Guo, S. B. Johnson, T. L. Campbell, H. Zhang, R. C. Vrijenhoek, F. P. Chavez, and J. Geller. 2020. Zooplankton biogeographic boundaries in the California current system as determined from metabarcoding. PloS One **15**: e0235159. doi:[10.1371/journal.pone.0235159](https://doi.org/10.1371/journal.pone.0235159)
- Pozo Buil, M., and others. 2021. A dynamically downscaled Ensemble of Future Projections for the California current system. Front. Mar. Sci. **8**.
- Ratnarajah, L., and others. 2023. Monitoring and modelling marine zooplankton in a changing climate. Nat. Commun. **14**: 564. doi:[10.1038/s41467-023-36241-5](https://doi.org/10.1038/s41467-023-36241-5)
- Ruzicka, J. J., R. D. Brodeur, R. L. Emmett, J. H. Steele, J. E. Zamon, C. A. Morgan, A. C. Thomas, and T. C. Wainwright. 2012. Interannual variability in the northern California current food web structure: Changes in energy flow pathways and the role of forage fish, euphausiids, and jellyfish. Prog. Oceanogr. **102**: 19–41. doi:[10.1016/j.pocean.2012.02.002](https://doi.org/10.1016/j.pocean.2012.02.002)
- Saint-Béat, B., G. Darnis, M. Leclerc, M. Babin, and F. Maps. 2022. Same mesozooplankton functional groups, different functions in three Arctic marine ecosystems. Funct. Ecol. **36**: 3161–3174. doi:[10.1111/1365-2435.14179](https://doi.org/10.1111/1365-2435.14179)

- Scheffer, M., and others. 2009. Early-warning signals for critical transitions. *Nature* **461**: 53–59. doi:10.1038/nature08227
- SIO-CalCOFI Technical Group. 2017. CalCOFI CTD Methods. SIO-CalCOFI Technical Group.
- Sommer, S. A., L. V. Woudenberg, P. H. Lenz, G. Cepeda, and E. Goetze. 2017. Vertical gradients in species richness and community composition across the twilight zone in the North Pacific subtropical gyre. *Mol. Ecol.* **26**: 6136–6156. doi:10.1111/mec.14286
- Steinberg, D. K., and M. R. Landry. 2017. Zooplankton and the ocean carbon cycle. *Ann. Rev. Mar. Sci.* **9**: 413–444. doi:10.1146/annurev-marine-010814-015924
- Takimoto, G., and D. M. Post. 2013. Environmental determinants of food-chain length: A meta-analysis. *Ecol. Res.* **28**: 675–681. doi:10.1007/s11284-012-0943-7
- Thomson, R. E., and M. V. Krassovski. 2010. Poleward reach of the California undercurrent extension. *J. Geophys. Res. Oceans* **115**. doi:10.1029/2010JC006280
- Valencia, B., M. Décima, and M. R. Landry. 2018. Environmental effects on Mesozooplankton size structure and export flux at station ALOHA, North Pacific subtropical gyre. *Global Biogeochem. Cycles* **32**: 289–305. doi:10.1002/2017GB005785
- Villarino, E., and others. 2018. Large-scale ocean connectivity and planktonic body size. *Nat. Commun.* **9**: 142. doi:10.1038/s41467-017-02535-8
- Whitmore, B. M., and M. D. Ohman. 2021. Zooglider-measured association of zooplankton with the fine-scale vertical prey field. *Limnol. Oceanogr.* **66**: 3811–3827. doi:10.1002/lno.11920
- Xiu, P., F. Chai, E. N. Curchitser, and F. S. Castruccio. 2018. Future changes in coastal upwelling ecosystems with global warming: The case of the California current system. *Sci. Rep.* **8**: 2866. doi:10.1038/s41598-018-21247-7
- Zhan, A., and others. 2013. High sensitivity of 454 pyrosequencing for detection of rare species in aquatic communities. *Methods Ecol. Evol.* **4**: 558–565. doi:10.1111/2041-210X.12037

Acknowledgments

Thanks to the California Current Ecosystem LTER program and the R/V *Sikuliaq* for sample collections. E. Tovar assisted with ZooScanning and H. Zheng with molecular analyses. The SIO Pelagic Invertebrate Collection provided access to zooplankton samples. Funding was provided by a US NSF Graduate Research Fellowship to S.A. Matthews, by National Science Foundation support to the California Current Ecosystem LTER site, and by Gordon and Betty Moore Foundation support to M.D. Ohman. We are grateful to the editors of the journal and two anonymous reviewers for suggestions for improving the manuscript.

Conflict of Interest

None declared.

Submitted 27 January 2023

Revised 30 August 2023

Accepted 14 October 2023

Associate editor: Thomas Kiørboe